
Since January 2020 Elsevier has created a COVID-19 resource centre with free information in English and Mandarin on the novel coronavirus COVID-19. The COVID-19 resource centre is hosted on Elsevier Connect, the company's public news and information website.

Microbial Pathogenesis 170 (2022) 105687

Contents lists available at ScienceDirect

Microbial Pathogenesis

journal homepage: www.elsevier.com/locate/micpath

# Evaluating the immunogenicity of gold nanoparticles conjugated RBD with Freund's adjuvant as a potential vaccine against SARS-CoV-2

Mahtab Moshref Javadi [a], Mozhgan Taghdisi Hosseinzadeh [a], Neda Soleimani [a,*], Foad Rommasi [b]

[a] Department of Microbiology and Microbial Biotechnology, Faculty of Life Sciences and Biotechnology, Shahid Beheshti University, Tehran, Iran
[b] Faculty of Life Sciences and Biotechnology, Shahid Beheshti University, Tehran, Iran

ARTICLE INFO

*Keywords:*
SARS-CoV-2
Gold nanoparticles
COVID-19 vaccine
RBD protein
Nano-vaccines
Immunogenic proteins
Freund's adjuvant

ABSTRACT

*Background:* and Introduction: SARS-CoV-2 is currently considered as the most challenging issue in the field of health and medicine by causing a global pandemic. Vaccines are counted as a promising candidate to terminate this deadly pandemic. Various structural proteins in SARS-CoV-2 have recently drawn attention to be utilized as candidate vaccines to stimulate immune responses against COVID-19.

*Materials and methods:* In current study, the RBD protein was cloned and expressed in *E. coli* host. Then, the expressed RBD protein was purified and its characterizations were evaluated through various methods. Gold nanoparticles, which were utilized as a carrier for candidate Nano-vaccine, were synthesized via oxidation-reduction reaction. While Gold NPs-conjugated RBD was injected into the second treatment group, in the first candidate vaccine, RBD was injected into the first treatment group solely. Complete and Incomplete Freud's Adjuvant were also utilized for both treatment groups to enhance the immune responses against RBD antigen. Immunizations were repeated 2 times in 14-day intervals to boost the immune system of BALB/c mice. The humoral and cell-mediated immune responses were examined through immune and cytokine assays.

*Results:* Our outcomes demonstrate that strong short-term humoral immunity (IgM) was induced in both the first and second treatment group, while long-term humoral responses (IgG) were only observed in the second treatment group. While stronger short- and long-term humoral (IgM and IgG, respectively) were observed in the second treatment group, particular cytokines production (TNF-α and IFN-γ) as a marker of cell-mediated responses were significantly higher in the first treatment group.

*Discussion and conclusion:* Our study results show the high potentiality of RBD protein as an appropriate stimulating antigen in vaccine synthesis and testifies RBD-based candidate vaccines to control the COVID-19 pandemic. Our outcomes also recommend that Nano-vaccines can be more suitable candidates when stronger long-term immune responses matter.

## 1. Introduction

SARS-CoV-2, now known as the newest member of the coronavirus family, was first identified in December 2019 in Wuhan city, Hubei Province, China [1]. Following the discovery of the virus in Wuhan, it was first introduced as 2019 novel coronavirus (2019-nCoV). On February 11, 2020, it was officially named SARS-CoV-2 by the World Health Organization (WHO) [2]. After SARS-CoV-2 spread, the WHO declared this virus outbreak as a pandemic at an official meeting on January 30, 2020 [3]. According to official statistics, as of 1 December 2021, a total of 263,808,200 people have been infected with the SARS CoV-2, of which 3,445,325 have passed away from coronavirus disease of 2019 (COVID-19) [4].

Phylogenetic studies have demonstrated that SARS-CoV-2 is a Beta coronavirus that has RNA as its genetic material [5,6]. In the external structure of the SARS-CoV-2, various proteins, including spike protein (S), Nucleocapsid protein (N), membrane protein (M), envelope protein (E), and hemagglutinin esterase (HE), are located [2]. The SARS-CoV-2 spike protein has a crucial role in the binding of the virus to host cells and causing infection. The spike protein is a homo-trimeric protein consisting of three identical monomers (each containing one subunit S1 and one subunit S2) [7]. Microscopic analysis has indicated that initial interactions are established between the S1 subunit and the

* Corresponding author.
*E-mail address:* N_soleimani@sbu.ac.ir (N. Soleimani).

https://doi.org/10.1016/j.micpath.2022.105687
Received 25 February 2022; Received in revised form 31 March 2022; Accepted 19 July 2022
Available online 31 July 2022

**Abbreviations**

Complete Freund's adjuvant CFA
Incomplete Freund's adjuvant IFA
Gold nanoparticles GNPs
Angiotensin-Converting Enzyme 2 ACE2
Receptor-binding domain RDB
Receptor-binding motif RBM
White blood cells WBCs
T helper cell type 1 Th1
T helper cell type 2 Th2
Interferon-γ IFN-γ
Tumor necrosis factor-α TNF-α
Interleukin-4 IL-4
Natural killer cells NK cells
Immunoglobulin Igs
Monophosphoryl lipid A MPLA
Scanning electron microscope SEM
Dynamic light scattering DLS
Ultraviolet–visible spectroscopy UV–Vis
Polymerase chain reaction PCR
Enzyme-linked immunosorbent assay ELISA
Sodium dodecyl sulfate polyacrylamide gel electrophoresis SDS-PAGE
Phosphate-buffered saline PBS
Diethylpyrocarbonate DEPC
Glyceraldehyde-3-Phosphate Dehydrogenase GAPDH
Isopropyl β-D-1-thiogalactopyranoside IPTG
Luria–Bertani LB
Housekeeping gene HKG
Intraperitoneal injection IP
Freund's Adjuvant FA
Hepatitis E virus HEV

Angiotensin-Converting Enzyme 2 (ACE2) receptor, promoting the transmission of the S2 subunit from metastable to more stable after fusion [8,9].

Moreover, binding of spike protein to ACE2 is an essential step in virus fusion to host cells. *In vitro* data have testified that the SARS-CoV-2 receptor-binding domain (RDB) can bind to ACE2 with a suitable affinity in the low nanomolar ranges, indicating the importance of this domain (present in the S1 subunit) in the initiation of the infection [10]. The SARS-CoV-2 RBD structure generally consists of 5 anti-parallel beta sheets called beta 1, beta 2, beta 3, beta 4, beta 7, which are interconnected by other spatial structures (loops and helixes). At the end of this structure is a receptor-binding motif (RBM) that binds to the N-terminal of the ACE2 protein helix, causing the initial attachments and interactions [1].

After SARS-CoV-2 entry to lung alveoli cells, innate and acquired immunity get activated against this pathogen which leads to and immunopathological patterns [11]. Lymphopenia, lymphocytes dysfunction and sudden changes in the number of white blood cells (WBCs) are some of immune patterns of COVID-19 infection [12,13]. As an instance, it is indicated that a remarkable reduction in the number of natural killer cells (NK cells), $CD8^+$ and $CD4^+$ T cells, basophils and eosinophils occurs [14,15] while neutrophils increase [11]. The concentration of pro-inflammatory cytokines and Immunoglobulin (Igs) have been observed to enhance in SARS family infections [16], which seems to occur due to the high immunogenicity of spike protein and specially RBD.

The RBD amino acid sequence has also been determined. Based on the SARS-CoV-2 spike protein composition, its weight was estimated to be about 27 kDa but laboratory data have revealed that the actual weight of RBD is about 34 kDa. This enormous weight difference indicates that the RBD protein is highly glycosylated by carbohydrate compounds [17,18]. The results of animal studies on mice and non-human primates suggest that vaccination of these animals using RBD can trigger synthesis of IgM and IgG in their body [19] and this issue has made RBD protein a potential candidate for vaccine production.

In order to enhance the efficacy and immunogenicity of candidate or final vaccines, various adjuvants like monophosphoryl lipid A (MPLA), Freund's adjuvant (FA) or Aluminum salts are added to vaccine mixture [20]. However, other compounds like Nano-carriers –some of which are composed of numerous excipients [21]– have recently drawn scientists' attention for vaccine manufacturing. Various Nano-carriers such as Gold nanoparticles (GNPs or AuNPs) are currently utilized as antigen carriers and adjuvants to improve the efficiency of manufactured vaccines [22]. GNPs, which are constantly used as an adjuvant in candidate vaccines [23], can be considered a suitable option among other Nano-carriers due to their properties. In other words, GNPs have been shown to increase the presentation of conjugated antigens to immune cells and specific immunization [24,25]. This research study ultimately aimed to examine the immunogenicity of GNP-conjugated RBD protein (along with Freund's Adjuvant as immunogenicity booster) and the immune response that it can stimulate as a possible vaccine candidate.

## 2. Materials and methods

In the following, used materials and adopted methods for conduction of this study will be expounded.

### 2.1. RBD protein synthesis and purification

The genome sequence of RBD protein as a part of SARS-CoV-2 spike protein was cloned (Tehran, Iran). Then, the synthesized sequence was inserted into the pET28a vector. The *E. coli (DE3)* strain was utilized as a host for the pET28a-RBD plasmid to express RBD protein. Two important restriction endonuclease enzymes, BamH I and Hind III, were applied to insert the pET28a-RBD plasmid into the *E. coli (DE3)* strain genome and manufacture the recombinant bacteria. The transformed bacteria were then cultured and screened on the liquid Luria–Bertani (LB) plate which contained 100 μg/mL kanamycin antibiotic to detect the positive colonies easily. The transformed bacteria culture was incubated in a rotary shaker incubator at 37 °C for approximately 4 h. The sequencing method was confirmed to confirm the presence of RBD protein in transformed bacteria culture. The turbidity of culture was constantly checked and when it obtains to 0.6–1 mM at 600 wavelengths (nm), 1 μM of Isopropyl β-D-1-thiogalactopyranoside (IPTG) (Fermentas Co., Lithuania) was employed to induce the recombinant plasmids. To validate the transformation of *E. coli DE3* by a pET28a-RBD plasmid, the electrophoresis method was adopted. The cell extraction of pET28a-RBD-transformed *E. coli DE3* colonies along with T7 promoter and T7 terminator primers were used for PCR, and after that, electrophoresis was performed of Agarose 1% gel. The nucleic acid sequence of the T7 promoter and T7 terminator primers were 5′TAATACGACTCACTATAGGG3′ and 5′ GCTAGTTATTGCTCAGCGG3′, respectively. After RBD protein synthesis, Ni-NTA (Sigma Aldrich, USA) was used in order to purify it.

### 2.2. RBD protein analysis

Sodium dodecyl sulfate polyacrylamide gel electrophoresis method (SDS-PAGE) was used for RBD protein analysis. SDS-PAGE is an

electrophoresis-based method in which protein subunits are separated based on their molecular weight. In this method, sodium dodecyl sulfate (SDS), an anionic compound, is utilized to equalize polypeptide subunits' electric charge on the surface. After establishing an electric current in the SDS-PAGE method, the protein subunits are separated based on the electric charge and form a linear pattern on the polyacrylamide gel. By comparing the formed pattern with reference subunits, the number of protein subunits and the molecular weight of each can be understood [26,27]. As stated, 12.5% polyacrylamide gel (in SDS-PAGE) at the voltage of 100 V was used to analyze the RBD protein properties and measure its expression. The 1 kb molecular weight marker (Thermo-Scientific Co, Iran) was utilized to determine the RBD protein subunit's weight. Finally, Coomassie brilliant blue G-250 color (Fermentas Co., Lithuania) was also employed to stain polyacrylamide gel [28,29]. Nickel reluctant resin (Ni-NTA affinity chromatography) (Sigma Aldrich, USA) was used to purify the expressed RBD protein. Eventually, dialysis PBS buffer was used for the removal of the imidazole groups from the purified RBD [30,31]. The results of SDS-PAGE of RBD protein are thoroughly explained in the result section.

### 2.3. Gold nanoparticles synthesis

Gold nanoparticles were synthesized by the method explained elsewhere [32]. Briefly, the synthesis method of Gold NPs was based on the oxidation-reduction reactions [33]. Shortly, 500 μl of $HAuCl_4$ (1%) (10 mg/ml) (Sigma, US) was added to 25 ml of Milli-Q water (Sigma, US). After heating the solution, 3 ml of $2H_2O$–$Na_3C_6H_5O_7$ (1%) (10 mg/ml) (Sigma, US) was added to the boiling solution. After 22 min, the color of the solution turned reddish, and the reaction stopped. The reddish solution was then taken to room temperature (25 °C), filtered through a 0.22 μm filter, and stored at 4 °C. To discuss the details, filtering synthesized GNPs affects their size distribution and prevents the presence of particles and substances which are larger than 0.22 μm in the final solution. The presence of large particles in the candidate vaccine may cause deleterious incident of large particles aggregation and defect the ultimate purpose of the vaccine; hence, we used 0.22 μm filter to prevent such an incident [34]. Moreover, using 0.22-μm filters is a standard method generally used to sterilize heat-sensitive solutions and remove potential dust, bacteria, and fungi pollution [35]. Therefore, utilization of a 0.22-μm pore size filter guarantees that GNPs solution is sterile and observed immune responses are exclusively against candidate vaccines authenticating our outcomes. The synthesized Gold NPs were examined by scanning electron microscopy (SEM), ultraviolet–visible spectroscopy (UV–Vis), and Dynamic light scattering (DLS). Since the absence of any ions, especially sodium ions, in the Gold NPs synthesis process is critical [36], all the containers and glassware used in the synthesis process were washed once with a 1% solution of hydrochloric or nitric acid and then rinsed with deionized water.

### 2.4. Attachment of gold nanoparticles to RBD protein

For this purpose, first, the pH of the Gold NPs solution was adjusted to basic state (pH = 8) by utilizing the KOH solution. After adjusting the pH of the Gold NPs solution on 8, 400 μl of recombinant RBD protein (containing 152 μg/ml) was added slowly and dropwise to the 1 ml of Gold NPs solution under sterile conditions. Then was added to, and the final solution was stirred for 1 h at 4 °C. Unbound proteins were isolated from the solution by centrifugation of Gold NPs (1700 g, 30 min) [33,37]. The stability of Gold NP-conjugated RBD was measured by adding 10% sodium chloride solution [38]. All of the characterization outcomes are fully expounded in the result section.

### 2.5. Animals and study trials

In this experiment, thirty 6- to 8-week-old inbred female BALB/c mice (with an average weight of 20–22 gr) were purchased from the Pasteur Institute of Tehran, Iran. The animals were kept for one week before the experiment in conditions with a relative humidity of 40–70%, applying 12 h light/dark cycles at 22–25 °C and standard feeding. All animal experiments were performed according to the published instructions of Shahid Beheshti University, Iran. During the study, all animals were kept standard and ethical condition.

### 2.6. In vivo assay and immunization

For immunization, mice were randomly divided into experimental and control groups (All groups included ten mice). Mice were infused three times at 14-day intervals through intraperitoneal (IP) injection. The total injected volume for each mouse was precisely 100 μl. RBD mixed with complete and incomplete Freund's Adjuvant (RBD-CFA or RBD-IFA), and Gold NPs-conjugated RBD mixed with Freund's Adjuvant (Gold NP-conjugated RBD with FA) were used for the first and second treatment group, respectively. The vaccination process was as follows:

1) First treatment group: 50 μl of recombinant RBD protein (containing 152 μg/ml RBD) plus 50 μl Complete Freund's Adjuvant (CFA) purchased from Sigma, (US) was administered to the first group for the priming injection at day 0. A solution with the same volume (100 μl) in which CFA was substituted with IFA (to prevent unintended side effects) was injected as the booster shots on days 14 and 28.
2) Second treatment group: Second treatment group received 75 μl Gold NPs-conjugated RBD (consists of 50 μl of recombinant RBD protein (152 μg/ml RBD) and 25 μl Gold NPs (with a concentration of 0.04 g/400 ml) mixed with 25 μl Complete Freund's Adjuvant (Sigma, US) for the first injection. As a booster for second and third immunization, a solution with the same volume and concentrations as the first dose in which IFA was used instead of CFA was injected into the second treatment group on days 14 and 28.
3) Third treatment group (control group): 100 μl of phosphate buffer saline (PBS) instead of candidate vaccine solution was injected to the control group on days 0, 14, and 28. No other immunogenic substance was injected into this group.

### 2.7. Collecting blood samples

In order to collect blood samples in each state, five mice of each group were randomly chosen and anesthetized by IP injection of xylazine-ketamine-PBS. Then, collected blood samples were stored at room temperature for 30 min and finally were centrifuged at 2000 g for 20 min to separate plasma from hematocrit. As stated, candidate vaccine injection was performed on days 0, 14, and 28. Blood samples were taken from the immunized and control group five days before immunization to obtain serum for the first examinations and analysis of immunological content. Mandibular blood samples were collected ten days after the first injection for IgM analysis and ten days after the last injection for measuring total IgG and IgG2a, IgG1. For evaluating the immune responses, serum samples of all groups were analyzed by an Enzyme-linked immunosorbent (ELISA) assay. The process of *in vivo* assay and immunization (Fig. 1-A), as well as Gold NPs-conjugated RBD protein (Fig. 1-B), are schematically illustrated in Fig. 1.

### 2.8. ELISA assay for antibody responses analysis

The Vaccine-specific antibody responses were ascertained by measuring synthesized immunoglobulins in immunized mice by using the enzyme-linked immunosorbent assay (ELISA) assay. Briefly, 96 wells of each ELISA plate (Greiner, Germany) were coated with 100 μl of recombinant RBD protein (10 μg/mL in Carbonate-Bicarbonate Buffer Solution (CBS buffer), pH = 9.6) and incubated overnight at ambient temperature. Precisely, PBS and CBS buffers which are prevalently used for the coating process in ELISA, differ in pH (7.4 vs. 9.6, respectively); however, it is proven that CBS buffer is more appropriate for coating

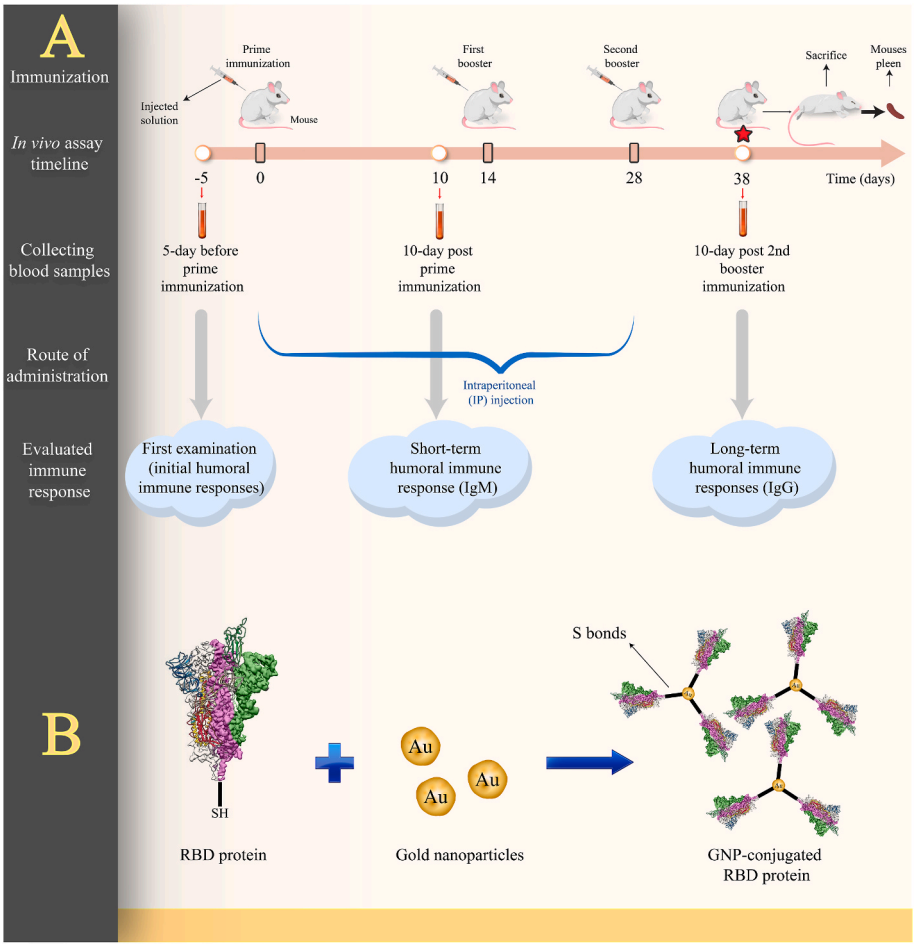


**Fig. 1.** The experiment process which was conducted in the current study: (A) A timeline of *in vivo* assay and immunization along with the route of administration, evaluated an immune response and ultimate purpose of collecting blood samples. (B) A schematic and straightforward figure about gold nanoparticles and RBD protein synthesis attachment reaction.

proteins and antigens in the ELISA procedure [39,40]. In fact, the higher pH of CBS strengthens the hydrophobic interactions among amino acid side chains and polystyrene of the plate; hence, it is widely used in ELISA protocol. Next, the ELISA plate was washed three times using PBS containing 0.05% Tween 20 (PBS-T as wash buffer) and was incubated with blocking buffer (containing 2–3% skim milk soluble in PBS buffer) at 37 °C for 2 h. The ELISA plates were then again washed three times with 250 μl PBS-T buffer 0.05% containing Tween 20 and 5 mM of $CaCl_2$ (as an eluting buffer). Collected mice sera as primary antibodies were diluted in ratios of 1:50–1:6400 using the serial dilution method and then were added to each well with 2% BSA in 1x PBS-T buffer and Tween 20. The ELISA plates were incubated with the described solution at 30 °C for 2 h. The plates were then washed five times with PBS-T buffer and incubated for 1 h at 37 °C with 100 μl of 1: 1000 diluted anti-mouse antibody conjugated to Horseradish Peroxidase (HRP, Sigma Aldrich, St Louis, MO, US). After washing the plates with PBS-T buffer, 100 μl of Tetramethylbenzidine (TMB, Sigma, US) liquid substrate was added to each well, and the plates were incubated in the dark ambiance for 30 min. Ultimately, the immune reaction was stopped by adding 100 μl of 2 M sulfuric acid ($H_2SO_4$) and the ELISA plate reader (Multiskan Lab systems) was used to read the absorbance of each ELISA plate at 450 nm (via The Beer-Lambert Law). The described method was also utilized for measuring the concentration of IgG isotypes through the indirect ELISA method in order to determine the type of immune responses (humoral or cellular). Literally, after the incubation of antigen coating overnight, the ELISA plates were eluted three times using 100 μl of PBS-T buffer. Then, 100 μL of the 1:10 diluted sere of immunized mice were added to each well. In the next step, 100 μl of 1:1000 anti-mouse IgG1, IgG2a, and IgM (as secondary Igs) were added to the ELISA wells which were previously washed three times by PBS-T buffer. After adding 100 μl of HRP-conjugated anti-gout antibody to each well and washing the plates, 100 TMB substrate was added to the plates. After incubating the plates in a dark ambiance for 30 min, 100 μl of 2 M sulfuric acid ($H_2SO_4$) was added to ELISA plates to stop the immune reactions. In the end, the ELISA plate reader (Multiskan Lab systems) was used to read the absorbance at 450 nm.

### 2.9. Cytokine assay by RT-PCR method

The innate immunity responses in immunized and control mice were assessed 10 days following the last injection by evaluating the concentration of IL-4, IFN-γ, and TNF-α and cytokines production. For this purpose, five mice were randomly selected from each group and got anesthetized by IP injection of xylazine-ketamine-PBS. They were sacrificed morally by observing ethic principles and their spleens were collected by considering ethical statement. Other mice were kept at standard conditions for evaluating the antibody responses to immunization. TRIzol reagent (Sigma, US) was used according to the manufacturer's instructions for RNA extraction from isolated spleens (~100 mg). DECP water (Sigma, US) was utilized for dissolving extracted mRNA from splenocytes. Then, the concentration of mRNA was determined by using a NanoDrop UV–vis spectrophotometer (Thermo ND-2000). The adsorption intensity of mRNA samples was read at 260 nm and the mRNA concentration was determined based on the measured

data. In order to eliminate or degrade any contaminating genomic DNA, the RNA solution was treated with DNase-I. A reagent kit (BIOFACT Co., Ltd) containing reverse-transcribed RNA enzyme was exploited for synthesizing cDNA from purified mRNAs. The transcription process took 15 min, and the temperature was set at 37 °C during the reaction. Finally, the transcription process was stopped by making a temperature shock (85 °C for 15 s). The synthesized cDNAs were then replicated by using polymerase chain reaction (PCR). DNA polymerase enzymes and thermal Cycler RT-PCR System (TaKaRa, Japan), which caused cDNA replication by crating multiple temperature cycles, was used for cDNA replication. Initially, the thermal cycler system was set to a temperature of 95 °C for 5 min to activate the enzyme DNA polymerase and break the hydrogen bonds between the cDNA strands. Then 40 two-step replication cycles (95 °C for 10 s and 60 °C for 30 s) were performed for enhancing the synthesized cDNA concentration. Finally, the thermal cycler device was set to 75 °C for 10 min to stop the PCR reaction. GAPDH as an endogenous housekeeping genes (HKG) was employed as an internal control. Then gene expression was evaluated by employing the $2^{-\Delta\Delta CT}$ method. The primer sets used to amplify the target cDNA were: IFN-γ (sense 5′- CAGCAACAGCAAGGCGAAAAAGG, antisense 5′- TTTCCGCTTCCTGAGGCTGGAT), TNF-α (sense 5′- GGTGCCTATGTCTCAGCCTCTT, antisense 5′- GCCATAGAACTGATGAGAGGGAG), IL-4 (sense 5′- ATCATCGGCATTTTGAACGAGGTC, antisense 5′- ACCTTGGAAGCCCTACAGACGA) and GAPDH (sense 5′- CATCACTGCCACCCAGAAGACTG, antisense 5′- ATGCCAGTGAGCTTCCCGTTCAG).

### 2.10. Statistical analysis

GraphPad Prism 8.0 (GraphPad Software, Inc., US), and SPSS 21.0 (SPSS, Inc, US) were utilized for statistical analysis of all data. All data are presented as mean ± standard error. Statistical significance was set to $P < 0.05$ (*), $P < 0.01$ (**), or $P < 0.001$ (***), $P < 0.0001$ (****) and they were interpreted as significant differences.

## 3. Results

### 3.1. Analysis of RBD protein properties

The RBD gene was initially inserted into plasmid pET28a as a carrier vector to synthesize the RBD protein. After embedding the RBD gene in the pET28a vector, the electrophoresis of colony-PCR product with T7 promoter and T7 terminator primers was performed on 1% Agarose gel to confirm the RBD gene presence in this vector. The result and Agarose 1% gel electrophoresis is illustrated in Fig. 2-A. Then, the recombinant plasmid (as a vector) was inserted into *E. coli (DE3)* by using bacterial transformation. Following the expression of RBD in modified *E. coli DE3*, RBD protein was purified using column Ni-NTA chromatography. In order to evaluate the molecular weight of synthesized RBD protein in plasmid pET28a -transformed *E. coli DE3*, bacterial cell extract supernatant was subjected to a 12.5% SDS-PAGE test. SDS-PAGE method confirmed the proper expression and purification of RBD protein. This test also determined the molecular weight of RBD protein 30 kDa and also the weight of one of its subunits. The SDS-PAGE gel is completely demonstrated in Fig. 2-B.

### 3.2. Characterization of Gold NPs-conjugated RBD

Gold nanoparticles were synthesized using an oxidation-reduction reaction following the instructions described in the method section. In this synthesis reaction, sodium citrate was employed as a reducing agent to reduce $HAuCl_4$. The synthesis of Gold NPs was confirmed by observing the change of the solution color to reddish. UV–vis, which was also utilized to test Gold NPs synthesis, confirmed the reaction incidence. The UV–vis results in Fig. 3-**B** indicated a strong absorption band at wavelength $\lambda_{max} = 525$ nm. SEM and DLS techniques were used to evaluate the structure, shape, and size of Gold NPs. The DLS and SEM results shown in Fig. 3-A & C, respectively revealed that the size of the synthesized Gold nanoparticles was about 50–60 nm.

The stability of Gold NPs-conjugated RBD was measured by adding 10% sodium chloride solution, which revealed the high stability of the synthesized Gold NPs-conjugated RBD (no alterations in color of the solution from reddish to blue and grey were observed). The synthesized compound was stored at ambient temperature for three weeks, and no physical or chemical discoloration was perceived, confirming the stability of Gold NPs-conjugated RBD.

### 3.3. ELISA assay for antibody responses analysis

As shown in Fig. 4 IgM and IgG titration (IgG1 and IgG2a subtypes) as markers of the humoral immune response. They also demonstrate the IgG1, IgG2a and IgM levels in the first treatment group (which only received RBD protein and Freund's adjuvant) and the second treatment group (which was treated with RBD-conjugated Gold NPs plus Freund's adjuvant) in comparison with the control group (in which only 100 μl of PBS was injected). To measure the short-term humoral immune response induced by immunization in each group, the concentration of IgM produced against RBD protein was measured by the indirect ELISA assay on the 10 day after the first immunization. The immunogenicity of the injected solution to each group was assessed by measuring the concentration of IgG1, IgG2a, IgG total antibodies produced against RBD protein in their serum by ELISA assay ten days after the last immunization. For evaluating antibodies concentration, ELISA plates were first coated by RBD protein (for RBD-specific antibody assay). After collecting blood samples, purified serum of each group was used for antibody measurement. The ELISA results in Fig. 4-**A** explicated that synthesized IgM in the first and second treatment groups was significantly higher than in the control group. However, produced IgM in the second treatment group was higher ($P < 0.0001$) than in the first treatment group ($P = 0.0001$). However, the amount of IgM produced in the second and first treatment groups was not significantly different. In Fig. 4-**B** the results of IgG1 measurement revealed that secretion of IgG1 in these two groups was remarkably higher than the control group. However, the level of

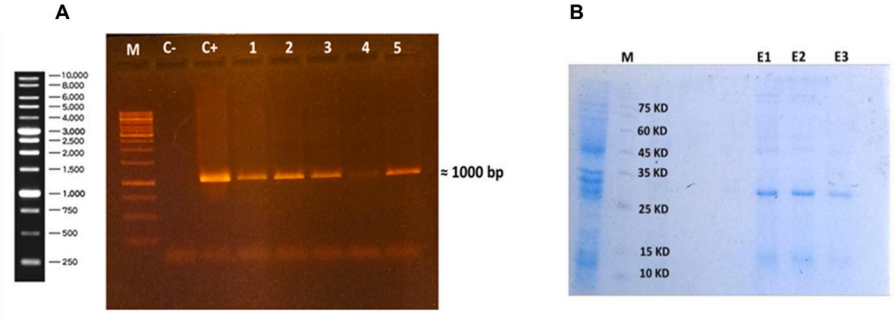


**Fig. 2. Results of electrophoresis colony-PCR product (A) and evaluation of protein expression RBD in 12.5% SDS-PAGE gel (B). Electrophoresis:** well M: Molecular Grower Marker (Thermo-Scientific Company, Iran); well C-: Negative control (no pattern DNA); C+ well: positive control (plasmid DNA pattern pET28a-RBD); 1 to 5 wells: Different transformed and cultured colonies (A). **SDS-PAGE:** well M: protein weight marker, Lane E1: Elution 1 of RBD protein after washing the affinity chromatography column, Lane E2: Elution 2 of RBD protein after washing the affinity chromatography column, Lane E3: Elution 3 of RBD protein after washing the affinity chromatography column. (B).

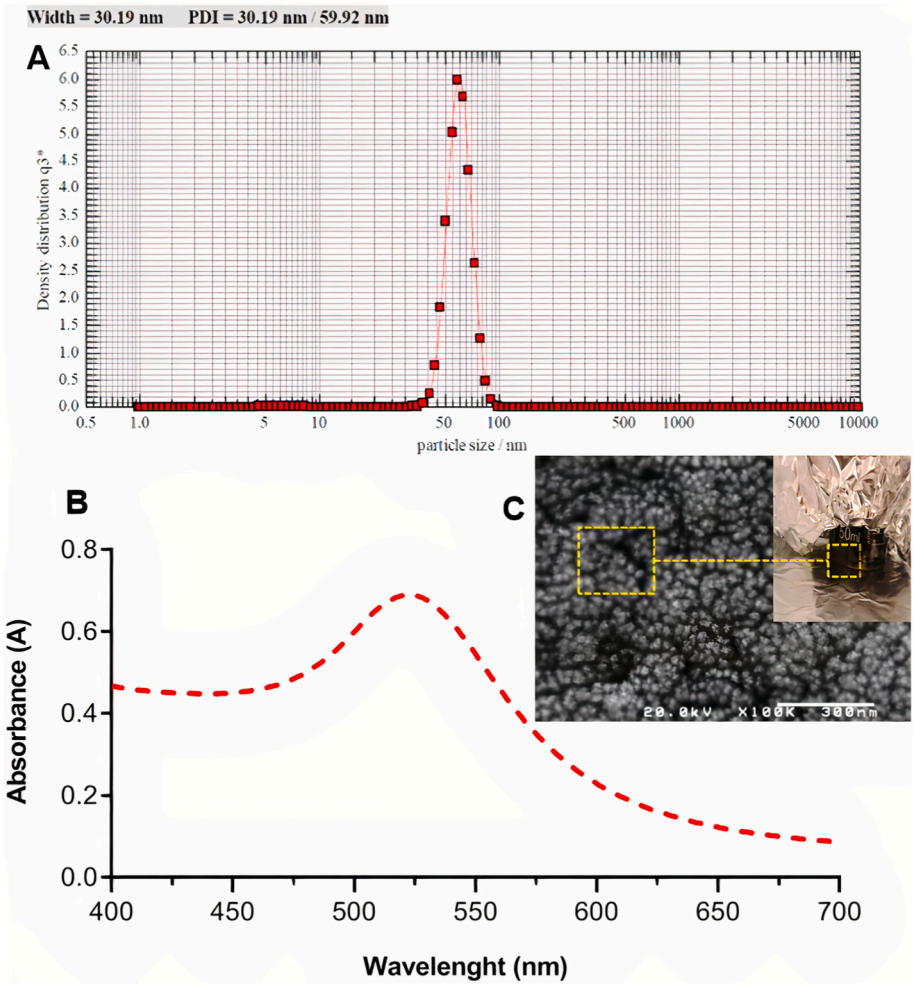


**Fig. 3. Characterization of Gold nanoparticles**. Gold NPs were synthesized following the procedure described. (A) dynamic light scattering (DLS); Polydispersity index (PDI) was 30.19 nm/59.92 nm (B) ultraviolet–visible spectroscopy (UV–Vis) and (C) scanning electron microscope (SEM); the scale bar of SEM was set to 300 nm.

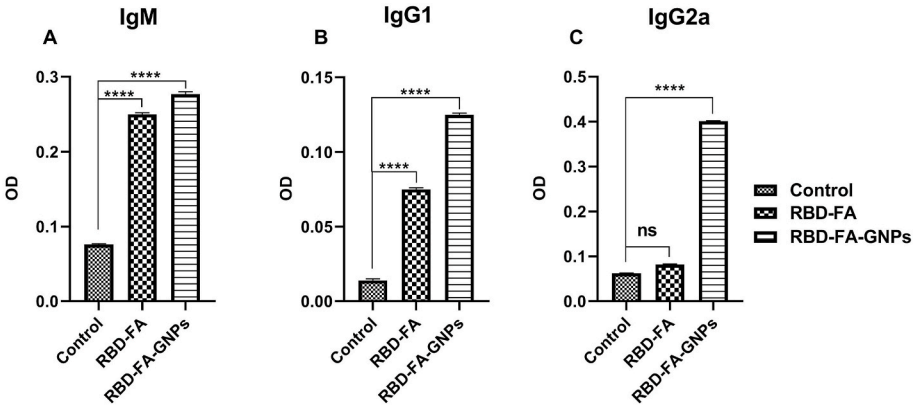


**Fig. 4. The effects of RBD immunization on levels of serum IgG isotypes (IgG1 as Th2-dependent isotype, IgG2a as Th1-biased IgG subclasses antibodies) and IgM.** The RBD plus Freund's adjuvant and Gold NPs was a potent inducer for IgM (A), IgG1 (B), and IgG2a (C) in comparison to the mice inoculated with PBS. All data are presented as mean ± standard error of the mean *p < 0.05, **p < 0.01, ***p < 0.001, ****p < 0.0001, N.S., not significant. (FA; Freund's Adjuvant, GNPs; Gold NPs).

IgG1 in the second treatment group was higher ($P = 0.0001$) than the first treatment group ($P = 0.0004$). As shown in Fig. 4-**C** there was no significant difference in the amount of IgG2a synthesized in the first treatment and control groups, proving the notable effect of applying Gold nanoparticles on the amount of IgG2a synthesis ($P < 0.0001$).

Eight various concentrations (including 1/50, 1/100, 1/200, 1/400, 1/800, 1/1600, 1/3200, and 1/6400) were prepared from the serum of immunized mice in the first and second treatment groups to validate the results. The concentration of total IgG in each group was determined using ELISA assay and absorption intensity. As shown in Fig. 5, the results revealed a significant immune response in the first group (RBD with Freund's adjuvant) and the second group (Gold NPs-conjugated RBD with Freund's Adjuvant) compared to the control group (PBS buffer). Although the endpoint titer of IgG total in the first group (1:800), and second group (1:1600), was significant compared to the control group. There was no significant difference in the endpoint titer of IgG total

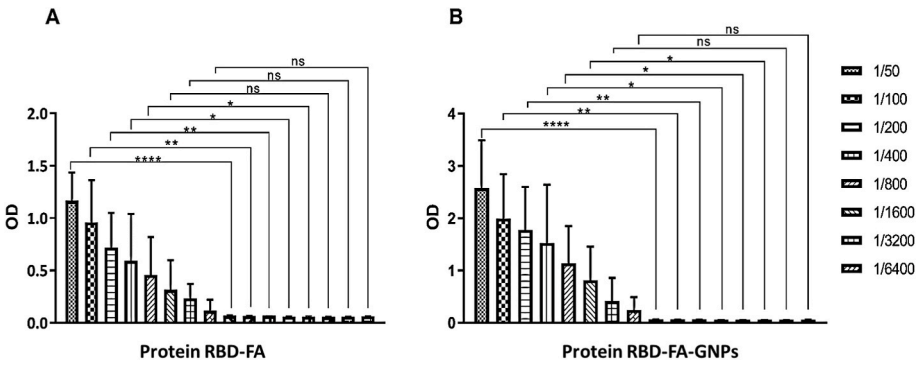


**Fig. 5. Analysis of total IgG antibody response to vaccine candidate.** The experimental groups of BALB/c mice (n = 10) were vaccinated i.p. With three doses of RBD- Freund's Adjuvant, RBD-Freund's adjuvant-Gold NPs, and PBS (control) on days 0, 14, and 28. (A) Immunogenicity analysis of the protein RBD-Freund's Adjuvant. (B) Immunogenicity analysis of the protein RBD-Freund's adjuvant-Gold NPs. Antibody titers were measured by the ELISA method. All data are presented as mean ± standard error of the mean *p < 0.05, **p < 0.01, ***p < 0.001, ****p < 0.0001, N·S., not significant.

antibody between the first and second groups (Fig. 5-A & B). These outcomes also confirmed that the application of Gold NPs-conjugated RBD with Freund's adjuvant compared to RBD protein with Freund's Adjuvant was associated with a more robust humoral immune response and higher IgG total synthesis.

### 3.4. Cytokines secretion and leucocytes proliferation

In order to evaluate the innate and cellular immune responses at the level of inflammatory molecules, ten days after the last immunization, five mice from each group were randomly selected and, after getting anesthetized by IP injection of xylazine-ketamine-PBS, were morally sacrificed. As mentioned, after isolating the spleen cell extract and synthesizing cDNA utilizing the mRNA splenocyte cell extract, the RT-PCR method was employed to measure the expression of three crucial cytokine genes, including IL-4, IFN-γ, and TNF-α. RT-PCR results (Fig. 6) displayed that the expression level of all measured cytokines (IL-4, IFN-γ, and TNF-α) was higher in the first treatment group (RBD-Freund's adjuvant) than in the second treatment group (RBD-Freund's adjuvant-Gold NPs) and control group (PBS). In Fig. 6-**B & C** the secretion of IFN-γ and TNF-α in RBD-Freund's adjuvant group was very significantly higher than the control group ($P < 0.0001$). In contrast, the expression of IFN-γ and TNF-α in the RBD-Freund's Adjuvant-Gold NPs and control group did not have meaningful differences and were almost similar. In Fig. 6-**B & C** the expression level of IFN-γ and TNF-α in RBD-Freund's Adjuvant-Gold NPs group than the control group was slightly increased ($P < 0.0004$) and non-significant (ns) respectively. In Fig. 6-**A**, the measurement of IL-4 expression, results showed that the expression of this cytokine in the first and second treatment groups was higher than in the control group ($P < 00001$, $P = 0.0001$) respectively.

In conclusion, immunized mice with RBD protein -Freund's Adjuvant displayed a high production of IFN-γ, TNF-α, and IL-4 that suggesting this group can effectively activate $CD4^+$ and $CD8^+$ T cells and balance Th1 and Th2 cellular responses. Interleukin-4 plays a vital role in the differentiation of naive T cells into Th2 as well as in the development of inflammatory responses. However, interferon-gamma is expressed in response to viral reactions.

## 4. Discussion

As stated, the novel beta coronavirus named SASR-CoV-2 was first detected in China and since then has spread all around the world and caused a global pandemic [41]. The virus structure is composed of RNA (as genetic material) and different proteins like the spike, nucleocapsid, etc., which can be exploited for therapeutic objectives. Due to the emergence of COVID-19 and its fast spread, it seems essential to control the pandemic through various strategies, but recently there has been no particular and effective medication [42]. Vaccines have always been one of the best tools for controlling contagious diseases such as BCG, smallpox, etc. That is why vaccines are currently suggested and utilized to prevent the deployment of COVID-19 and cut the transmission chain of SARS-CoV-2 [43]. In the past, vaccines were synthesized using traditional methods such as killing, attenuating, inactivating, or genetically modifying pathogens or other microorganisms [44]. Nowadays, various kinds of COVID-19 vaccines have been developed by using different and even novel methods such as highly-purifying antigens, transcriptable DNA, or mRNAs. mRNA-based, non-replicating viral vector, DNA-based, and subunit-based vaccines are some instances of SARS-CoV-2 vaccines currently available in the market and used publicly [45]. However, it appears the subunit-based vaccines are safer than whole-virion vaccines because of less exposure to the virus during manufacturing [42]. Recombinant protein-based and Nano-vaccines are also designed and developed due to the urgent requirement to manufacture efficient vaccines against new variants of SARS-CoV-2 [46].

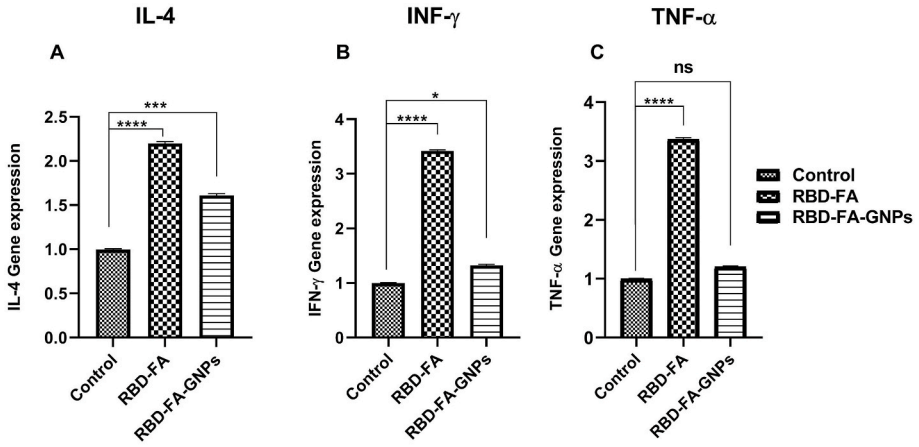


**Fig. 6. Cytokine release of mouse splenocytes stimulated by different components.** Level of IL-4 (A), IFN-γ (B), and TNF-α (C) secretion was evaluated in mouse splenocytes stimulated by RBD protein along with Freund's adjuvant and Gold NPs. The level of responses was evaluated ten days after the final immunization. Data represented the mean ± standard deviation of ten mice per group (n = 10). Statistical analysis was performed using the T-test (GraphPad Prism8) and statistical significance was set at *p ≤ 0.05; **p ≤ 0.01; ***p ≤ 0.001; ****p ≤ 0.0001. n.s. Non-significant. (FA; Freund's Adjuvant, GNPs; Gold NPs).

According to promising reports on their utilization, diverse nanoparticles such as liposomes, micelles, and polymer or Gold NPs-conjugated compounds have been tested as therapeutic agents or Nano-vaccines delivery devices [47]. Application of Nano-vaccines as new vaccine candidates may improve the induced immunity by delivering antigens specifically to B cell receptors, enhancing the cross-linked reactions, and increasing the immune system's ability to identify conjugated antigens [48]. As aforesaid, spike protein and its subunits, S1 and S2 proteins, in SARS-CoV-2 [49] can be widely used for designing recombinant or Nano-vaccines. It is testified that RBD that is present S1 domain of SARS-CoV-2 can induce remarkable immune responses when utilized as an immunogen substance in the vaccine [50].

In the present research, we have designed two different candidate vaccines and evaluated their immunogenicity. We also analyzed the immune responses which were induced following the injection of the candidate vaccines. The first candidate vaccine was a Nano-vaccine in which Gold NPs-conjugated RBD plus Freund's Adjuvant was prepared through reduction-oxidation reaction as described somewhere else [51]. The second candidate vaccine was based on the infusion of RBD protein itself as an antigen with Freund's Adjuvant for strengthening the triggered immune response. There was also a control group (which only received PBS buffer) for validating and comparing the outcomes. Our results testified that RBD protein has a crucial antigenicity and can be used for vaccine manufacturing. For preparing candidate vaccines in this study, recombinant RBD protein was synthesized by following the standard recombinant proteins method, including recombinant vector production, genome insertion, bacterial expression, and protein purification. Ultimately, the isolated and purified RBD recombinant protein concentration was evaluated, which determined adequate purity [52]. Gold NPs were synthesized through a reduction-oxidation reaction and utilized as a conjugate for RBD protein for preparation of Nano-vaccine due to its appropriate properties such as biocompatibility, non-cytotoxicity, and adjuvanticity characteristics [36,53]. The synthesized RBD protein was then conjugated to Gold NPs for preparing the first candidate vaccine, and control methods approved the formation of Gold NPs-conjugated RBD.

As mentioned, adjuvants are essential for enhancing the potential immunogenicity of the injected compound and improving the innate and acquired (humoral or cellular) responses to RBD protein. That is why we use complete and incomplete Freund's Adjuvant, which is one of the most potent oil-derived substances with adjuvant activity, to trigger immune responses more [54,55]. Immunization in the first and second treatment, as well as control group, was performed at Day 0 as priming and Day 14 and 28 as boosting doses by injecting prepared solution IP. Our outcomes illustrate that IgM and IgG total (including IgG1 and IgG2a subtypes) titer was significantly higher in the first treatment group (which received Gold NPs-conjugated RBD plus FA) the second treatment group (immunized by free RBD protein with FA) (Fig. 4). It testifies that the application of Gold NPs can be accompanied by high stimulation of humoral immunity. The expression of cytokine genes, which is commonly interpreted as activation of innate and acquired cellular immunity, was more in the second treatment group than the first treatment group (Fig. 6). It shows that the employment of RBD protein and FA may result in higher induction of cellular immunity according to our results.

Nanoparticles have been used as appropriate gadgets for cancer treatment, drug delivery, and vaccine synthesis. Nanoparticles usage for vaccine production has been demonstrated to increase the stability of conjugated substances (i.e., antigens) and improve the antigen process pathways [33,56]. Among various nanoparticles, Gold NPs are one of the best options as Nano-carriers for synthesizing Nano-vaccines according to their suitable attributes such as nontoxicity and biocompatibility [53].

There are various studies and experimental research in which the association of the active compounds with the Nano-systems, particularly GNPs, have been evaluated. As an example, Dakterzada et al. [57] used GNPs as an adjuvant along with *Pseudomonas aeruginosa* flagellin to induce immune reactions against *Pseudomonas aeruginosa*. Their results indicated high antibody production, significant cellular uptake of antigen, and no harmful immunogenicity or toxicity for GNPs themselves [57]. In another study conducted by Tao et al. [56], the exploitation of GNPs-conjugated M2e with CpG as an adjuvant was accompanied by remarkable humoral immune responses, particularly in IgG synthesis [56]. An *in vivo* study by Li et al. [33] demonstrated that utilizing GNPs can also activate innate and cellular immune responses against immunogens by increasing phagocytosis, lymphocytes proliferation and cytokine productions (IFN and IL-10 cytokines) [33]. It is also proven that GNPs are capable of fortifying $CD4^+$ and $CD8^+$ T cells and enhancing cytokines production in another study aiming at using NPs as carriers in a potential vaccine [58]. All in all, these studies are only a few instances of association of the active compounds with the Nano-system that elucidates the efficiency of applying GNPs as a novel technology for vaccine production and validates our results.

As our results testified, Gold NPs can improve the immunogenicity of antigens. They are also able to bind to various substances and antigens by strong chemical bonds, including hydrophilic or hydrophobic interactions [33], and their synthesis and attachment reaction is not complicated or dangerous. Gold NPs have also been utilized as Nano-carrier or adjuvants in other studies [57]. For instance, gold NPs were exploited in Hepatitis E virus (HEV) vaccine manufacturing by Dibya Rani et al. [59] which their results exhibit a remarkably robust humoral (IgG) and cell-mediated immune responses to candidate vaccine. Gold NPs have been shown to be able to influence the APCs (such as dendritic cells, Mast cells, and macrophages) and elevate the absorption and presentation of conjugated antigen to B and T cells. It is also testified that utilization of Gold NPs can be accompanied by an increase in mitochondrial activity of macrophages [60,61]. Our results demonstrate that Gold NPs can enhance the activity of B cells and, as a result, increase IgG and IgM production. These cases, along with promising outcomes of numerous conducted research that has used Gold NPs as carrier nanoparticles [22], validate its efficacy. That is why we've suggested and used Gold NPs-conjugated RBD as one of the crucial vaccine candidates.

Due to the potentially low immunogenicity of some antigens, particular components named adjuvants are usually used during immunization or vaccination by some antigens. The utilization of adjuvants can improve immunological tolerance as well [62,63]. Various substances, including organic ions, small molecules, and even some microbial-based materials, can be employed as adjuvants during immunization [64]. Freund's Adjuvant, which counts as a mycobacterial substance, is a lipid component and one of the strongest adjuvants [65]. Two different forms of Freund's Adjuvant known as CFA and IFA have various impacts on the immune system and stimulate diverse immunological responses. As an instant, CFA can activate antigen presentation pathways by dendritic cells and influence cellular immunity, while IFA has been proven to contribute to immunological tolerance induction [66,67]. It is reported that CFA seems to influence Th1 preferably and results in long-lasting immunity, while IFA is likely able to induce Th2 and related mechanisms [63]. Th1 is responsible for the synthesis of IFN-γ and IL-12 and is commonly associated with cellular immunity [68]. In contrast, IL-4, IL-10, and IL-5 are produced by Th2, and this type of T cell is related to humoral immunity [69]. In this study, we employ CFA and IFA both to balance the cellular and humoral responses to candidate vaccines. CFA was utilized for the priming immunization, while for booster immunizations, IFA was injected to treatment groups.

To recapitulate, two crucial topics (toxicity of GNPs and their pros against current solutions) need to be discussed. In terms of cytotoxicity, it is worth noting that GNPs toxicity on cells, remarkably immune cells such as dendritic cells (DCs), is primarily determined by their size and concentration [70]. To be precise, although smaller AuNPs have a more durable presence in blood circulation and better bio-distribution, they can much more easily penetrate cells and accumulate in cellular organelles, namely nuclei, causing deleterious impacts on DNA and cell

functionalization. On the other hand, it is testified that the increase of GNPs concentration in solution induces toxic effects on DCs [71,72]. The synthesized GNPs in this study were 50–60 nm in terms of size, and their concentration in injected solution was set to 100 μg/ml, which is highly safe for all cells, according to various articles [70–72].

To talk about the advantages of using nanotechnology over other existing solutions for vaccine production, it should be mentioned that amongst all type of traditional vaccines, subunit vaccine has gained lots of attraction currently due to their safety and easy production; however, easy degradation, acting as PAMP due to the lack of whole virus components and low immunogenicity is some examples of its disadvantages [73,74]. In contrast, as our outcomes demonstrate, AuNPs have remarkable immunogenicity when used with an antigen enabling them to be applied as a robust antigen carrier or Adjuvant. Moreover, Nano-systems, particularly GNPs, are able to be used in various ways, including intranasal and intestinal, since they can pass through intestinal space [75]. Having the high potential of being conjugated to DNA, RNA and protein [76], specific targeting and diminished adverse effects of off-target [77], sustained releasing of loaded compound [78], and remarkable effect for stimulating both humoral and cellular immune responses simultaneously [47] are the other pros of GNPs as a representative of Nano-systems over other existing solutions for COVID-19 vaccine synthesis [76]. These items show the importance of substituting old methods with novel strategies for vaccine production and highlight the affective impacts of GNPs over other solutions.

## 5. Conclusion

In short, we used two various candidate vaccines for immunization of BALB/c mice by employing the RBD sequence of the spike protein of SARS-CoV-2 as the main compound of both candidate vaccines. Our results showed that Gold NPs could be an appropriate Nano-carrier due to its unique properties and ability to improve antibody production enormously. We also utilized complete and incomplete Freund's Adjuvant to boost the immune responses, which caused robust cellular and innate immune responses (especially in cytokine production). Both candidate vaccines show promising and appropriate activity in immunization against SARS-CoV-2. It should also be noted that RBD protein has a crucial rule in SARS-CoV-2 entry to host cells; therefore, vaccines that specifically render immunity against this part of spike protein may provide powerful immunity against COVID-19. This powerful immunity can be improved by applying Gold NPs and Freund's Adjuvant. The results of our study could create new horizons for the use of nanoparticles in the production of the COVID-19 vaccine and while helping to control the pandemic, draw the attention of scientists to this critical issue. Despite all progress, there is still a great demand to study and instigate SARS-CoV-2 and its properties to control the current deadly pandemic. Future research should consider new candidate vaccines due to their essential role in controlling the COVID-19 pandemic.

## Authors' contributions

MMJ, MT, and NS contributed to the conceptualization and performing research. MMJ and FR contributed to the investigations. FR prepared the main manuscript and contributed to the writing-original draft completely, and figures preparation. MMJ and FR performed edition and reviewing. All authors read the manuscript intently and approved its content.

## Ethical approval

All experiments and animal studies were conducted according to guidelines approved by Animal Ethics committee of Shahid Beheshti University. This research was approved by the Shahid Beheshti University under the ethical code IR.SBU/493/1399D.

## Availability of materials and data

No datasets were generated or analyzed during the current study. All data are available in the article.

## CRediT authorship contribution statement

**Mahtab Moshref Javadi:** Methodology, Investigation, Formal analysis. **Mozhgan Taghdisi Hosseinzadeh:** Methodology, Investigation, Formal analysis. **Neda Soleimani:** Supervision, Project administration, Conceptualization. **Foad Rommasi:** Writing – original draft, Visualization, Validation.

## Declaration of competing interest

The authors declare that they have no competing interests.

## Data availability

No data was used for the research described in the article.

## Acknowledgements

Not applicable.

## References

[1] J. Lan, J. Ge, J. Yu, S. Shan, H. Zhou, S. Fan, Q. Zhang, X. Shi, Q. Wang, L. Zhang, Structure of the SARS-CoV-2 spike receptor-binding domain bound to the ACE2 receptor, Nature 581 (7807) (2020) 215–220.
[2] P. Zhou, X.-L. Yang, X.-G. Wang, B. Hu, L. Zhang, W. Zhang, H.-R. Si, Y. Zhu, B. Li, C.-L. Huang, A pneumonia outbreak associated with a new coronavirus of probable bat origin, Nature 579 (7798) (2020) 270–273.
[3] Jebril, N., World Health Organization Declared a Pandemic Public Health Menace: A Systematic Review of the Coronavirus Disease 2019 "COVID-19", up to 26th March 2020. Available at: SSRN 3566298 2020.
[4] Worldmeters Coronavirus update. https://www.worldometers.info/coronavirus/(accessed 01 December 2021).
[5] C.I. Paules, H.D. Marston, A.S. Fauci, Coronavirus infections—more than just the common cold, JAMA 323 (8) (2020) 707–708.
[6] F. Li, W. Li, M. Farzan, S.C. Harrison, Structure of SARS coronavirus spike receptor-binding domain complexed with receptor, Science 309 (5742) (2005) 1864–1868.
[7] F. Salamanna, M. Maglio, M.P. Landini, M. Fini, Body localization of ACE-2: on the trail of the keyhole of SARS-CoV-2, Front. Med. 7 (2020) 935.
[8] R.N. Kirchdoerfer, N. Wang, J. Pallesen, D. Wrapp, H.L. Turner, C.A. Cottrell, K. S. Corbett, B.S. Graham, J.S. McLellan, A.B. Ward, Stabilized coronavirus spikes are resistant to conformational changes induced by receptor recognition or proteolysis, Sci. Rep. 8 (1) (2018) 1–11.
[9] Y. Yuan, D. Cao, Y. Zhang, J. Ma, J. Qi, Q. Wang, G. Lu, Y. Wu, J. Yan, Y. Shi, Cryo-EM structures of MERS-CoV and SARS-CoV spike glycoproteins reveal the dynamic receptor binding domains, Nat. Commun. 8 (1) (2017) 1–9.
[10] X. Tian, C. Li, A. Huang, S. Xia, S. Lu, Z. Shi, L. Lu, S. Jiang, Z. Yang, Y. Wu, Potent binding of 2019 novel coronavirus spike protein by a SARS coronavirus-specific human monoclonal antibody, Emerg. Microb. Infect. 9 (1) (2020) 382–385.
[11] L. Yang, S. Liu, J. Liu, Z. Zhang, X. Wan, B. Huang, Y. Chen, Y. Zhang, COVID-19: immunopathogenesis and Immunotherapeutics, Signal Transduct. Targeted Ther. 5 (1) (2020) 1–8.
[12] L. Tan, Q. Wang, D. Zhang, J. Ding, Q. Huang, Y.-Q. Tang, Q. Wang, H. Miao, Lymphopenia predicts disease severity of COVID-19: a descriptive and predictive study, Signal Transduct. Targeted Ther. 5 (1) (2020) 1–3.
[13] Y. Liu, W. Sun, J. Li, L. Chen, Y. Wang, L. Zhang, L. Yu, Clinical features and progression of acute respiratory distress syndrome in coronavirus disease 2019, medRxiv (2020), https://doi.org/10.1101/2020.02.17.20024166v3.
[14] Z. Xu, L. Shi, Y. Wang, J. Zhang, L. Huang, C. Zhang, S. Liu, P. Zhao, H. Liu, L. Zhu, Pathological findings of COVID-19 associated with acute respiratory distress syndrome, Lancet Respir. Med. 8 (4) (2020) 420–422.
[15] C. Huang, Y. Wang, X. Li, L. Ren, J. Zhao, Y. Hu, L. Zhang, G. Fan, J. Xu, X. Gu, Clinical features of patients infected with 2019 novel coronavirus in Wuhan, China, Lancet 395 (10223) (2020) 497–506.
[16] C.K.-f. Li, H. Wu, H. Yan, S. Ma, L. Wang, M. Zhang, X. Tang, N.J. Temperton, R. A. Weiss, J.M. Brenchley, T cell responses to whole SARS coronavirus in humans, J. Immunol. 181 (8) (2008) 5490–5500.
[17] Q. Wang, J. Qi, Y. Yuan, Y. Xuan, P. Han, Y. Wan, W. Ji, Y. Li, Y. Wu, J. Wang, Bat origins of MERS-CoV supported by bat coronavirus HKU4 usage of human receptor CD26, Cell Host Microbe 16 (3) (2014) 328–337.
[18] K. Xiao, Z. Tian, GPSeeker enables quantitative structural N-glycoproteomics for site-and structure-specific characterization of differentially expressed N-

glycosylation in hepatocellular carcinoma, J. Proteome Res. 18 (7) (2019) 2885–2895.
[19] J. Yang, W. Wang, Z. Chen, S. Lu, F. Yang, Z. Bi, L. Bao, F. Mo, X. Li, Y. Huang, A vaccine targeting the RBD of the S protein of SARS-CoV-2 induces protective immunity, Nature 586 (7830) (2020) 572–577.
[20] C.R. Alving, G.R. Matyas, O. Torres, R. Jalah, Z. Beck, Adjuvants for vaccines to drugs of abuse and addiction, Vaccine 32 (42) (2014) 5382–5389.
[21] Y. Wang, M. Beck-Broichsitter, M. Yang, J. Rantanen, A. Bohr, Investigation of nanocarriers and excipients for preparation of nanoembedded microparticles, Int. J. Pharm. 526 (1–2) (2017) 300–308.
[22] L. Dykman, S. Staroverov, V. Bogatyrev, S.Y. Shchyogolev, Adjuvant properties of gold nanoparticles, Nanotechnol. russia 5 (11) (2010) 748–761.
[23] J.A. Salazar-González, O. Gonzalez-Ortega, S. Rosales-Mendoza, Gold nanoparticles and vaccine development, Expet Rev. Vaccine 14 (9) (2015) 1197–1211.
[24] K. Fytianos, L. Rodriguez-Lorenzo, M.J. Clift, F. Blank, D. Vanhecke, C. Von Garnier, A. Petri-Fink, B. Rothen-Rutishauser, Uptake efficiency of surface modified gold nanoparticles does not correlate with functional changes and cytokine secretion in human dendritic cells in vitro, Nanomed. Nanotechnol. Biol. Med. 11 (3) (2015) 633–644.
[25] X. Le Guével, F. Palomares, M.J. Torres, M. Blanca, T.D. Fernandez, C. Mayorga, Nanoparticle size influences the proliferative responses of lymphocyte subpopulations, RSC Adv. 5 (104) (2015) 85305–85309.
[26] H. Schägger, Tricine–sds-page, Nat. Protoc. 1 (1) (2006) 16–22.
[27] A.A. Al-Tubuly, SDS-PAGE and western blotting, in: Diagnostic and Therapeutic Antibodies, Springer, 2000, pp. 391–405.
[28] J. Liu, C. He, M. Chen, Z. Wang, C. Xing, Y. Yuan, Association of presence/absence and on/off patterns of Helicobacter pylori oipA gene with peptic ulcer disease and gastric cancer risks: a meta-analysis, BMC Infect. Dis. 13 (1) (2013) 1–10.
[29] N. Soleimani, B. Farhangi, M.T. Yaraki, The effect of recombinant HopH protein of Helicobacter pylori on the VEGF expression in metastatic breast cancer model, Acta Med. Iran. (2017) 744–750.
[30] P.T. Wingfield, Overview of the purification of recombinant proteins, 6.1. 1-6.1. 35, Curr. Protoc. Protein Sci. 80 (1) (2015).
[31] R.C. Akhani, A.T. Patel, M.J. Patel, S.R. Dedania, J.S. Patel, D.H. Patel, Column chromatography free purification of recombinant α-amylase from bacillus licheniformis by tagging with hydrophobic elastin like polypeptide, Proc. Natl. Acad. Sci. India B Biol. Sci. 88 (3) (2018) 1249–1255.
[32] J. Kimling, M. Maier, B. Okenve, V. Kotaidis, Ballot, A. Plech, J. Phys. Chem. B 110 (2006) 15700–15707.
[33] Y. Li, Q. Jin, P. Ding, W. Zhou, Y. Chai, X. Li, Y. Wang, G. Zhang, Gold nanoparticles enhance immune responses in mice against recombinant classical swine fever virus E2 protein, Biotechnol. Lett. 42 (7) (2020) 1169–1180.
[34] T. Arakawa, J.S. Philo, D. Ejima, K. Tsumoto, F. Arisaka, Aggregation analysis of therapeutic proteins, part 2, Bioproc. Int. 5 (4) (2007) 36–47.
[35] S.E. Walsh, S.P. Denyer, Filtration sterilization. Russell, hugo & ayliffe's: principles and practice of disinfection, Preserv. Steriliz. (2013) 343–370.
[36] S. Farfán-Castro, M.J. García-Soto, M. Comas-García, J.I. Arévalo-Villalobos, G. Palestino, O. González-Ortega, S. Rosales-Mendoza, Synthesis and immunogenicity assessment of a gold nanoparticle conjugate for the delivery of a peptide from SARS-CoV-2, Nanomed. Nanotechnol. Biol. Med. 34 (2021), 102372.
[37] W. Haiss, N.T. Thanh, J. Aveyard, D.G. Fernig, Determination of size and concentration of gold nanoparticles from UV− Vis spectra, Anal. Chem. 79 (11) (2007) 4215–4221.
[38] S. Lou, J.-y. Ye, K.-q. Li, A. Wu, A gold nanoparticle-based immunochromatographic assay: the influence of nanoparticulate size, Analyst 137 (5) (2012) 1174–1181.
[39] L. Zhang, X. Du, C. Chen, Z. Chen, L. Zhang, Q. Han, X. Xia, Y. Song, J. Zhang, Development and characterization of double-antibody sandwich ELISA for detection of Zika virus infection, Viruses 10 (11) (2018) 634.
[40] N. Xu, C. Qu, W. Ma, L. Xu, L. Xu, L. Liu, H. Kuang, C. Xu, Development and application of one-step ELISA for the detection of neomycin in milk, Food Agric. Immunol. 22 (3) (2011) 259–269.
[41] J. Tao, Y. Ma, C. Luo, J. Huang, T. Zhang, F. Yin, Summary of the COVID-19 epidemic and estimating the effects of emergency responses in China, Sci. Rep. 11 (1) (2021) 1–9.
[42] Y. Wang, L. Wang, H. Cao, C. Liu, SARS-CoV-2 S1 is superior to the RBD as a COVID-19 subunit vaccine antigen, J. Med. Virol. 93 (2) (2021) 892–898.
[43] A. Koirala, Y.J. Joo, A. Khatami, C. Chiu, P.N. Britton, Vaccines for COVID-19: the current state of play, Paediatr. Respir. Rev. 35 (2020) 43–49.
[44] M.J. Saadh, H.M. Sbaih, A. Mustafa, B.A. Alawadie, M. Abunuwar, M. Aldhoun, B. Al-jaidi, Whole-organism vaccine (attenuated and killed vaccines), J. Chem. Pharmaceut. Res. 9 (10) (2017) 1–4.
[45] A. Kumar, W.E. Dowling, R.G. Román, A. Chaudhari, C. Gurry, T.T. Le, S. Tollefson, C.E. Clark, V. Bernasconi, P.A. Kristiansen, Status report on COVID-19 vaccines development, Curr. Infect. Dis. Rep. 23 (6) (2021) 1–12.
[46] T. Yadav, N. Srivastava, G. Mishra, K. Dhama, S. Kumar, B. Puri, S.K. Saxena, Recombinant vaccines for COVID-19, Hum. Vaccines Immunother. 16 (12) (2020) 2905–2912.
[47] G. Chauhan, M.J. Madou, S. Kalra, V. Chopra, D. Ghosh, S.O. Martinez-Chapa, Nanotechnology for COVID-19: therapeutics and vaccine research, ACS Nano 14 (7) (2020) 7760–7782.
[48] P. Ding, T. Zhang, Y. Li, M. Teng, Y. Sun, X. Liu, S. Chai, E. Zhou, Q. Jin, G. Zhang, Nanoparticle orientationally displayed antigen epitopes improve neutralizing antibody level in a model of porcine circovirus type 2, Int. J. Nanomed. 12 (2017) 5239.
[49] L. Guruprasad, Human SARS CoV-2 spike protein mutations, Proteins: Struct., Funct., Bioinf. 89 (5) (2021) 569–576.
[50] S. Ravichandran, E.M. Coyle, L. Klenow, J. Tang, G. Grubbs, S. Liu, T. Wang, H. Golding, S. Khurana, Antibody signature induced by SARS-CoV-2 spike protein immunogens in rabbits, Sci. Transl. Med. 12 (550) (2020).
[51] J. Kimling, M. Maier, B. Okenve, V. Kotaidis, H. Ballot, A. Plech, Turkevich method for gold nanoparticle synthesis revisited, J. Phys. Chem. B 110 (32) (2006) 15700–15707.
[52] M.H. Lew, M.N. Norazmi, G.J. Tye, Enhancement of immune response against Mycobacterium tuberculosis HspX antigen by incorporation of combined molecular adjuvant (CASAC), Mol. Immunol. 117 (2020) 54–64.
[53] R. Shukla, V. Bansal, M. Chaudhary, A. Basu, R.R. Bhonde, M. Sastry, Biocompatibility of gold nanoparticles and their endocytotic fate inside the cellular compartment: a microscopic overview, Langmuir 21 (23) (2005) 10644–10654.
[54] J.C. Chang, J.P. Diveley, J.R. Savary, F.C. Jensen, Adjuvant activity of incomplete Freund's adjuvant, Adv. Drug Deliv. Rev. 32 (3) (1998) 173–186.
[55] A.M. Dvorak, H. Dvorak, Structure of Freund's complete and incomplete adjuvants: relation of adjuvanticity to structure, Immunology 27 (1) (1974) 99.
[56] W. Tao, K.S. Ziemer, H.S. Gill, Gold nanoparticle–M2e conjugate coformulated with CpG induces protective immunity against influenza A virus, Nanomedicine 9 (2) (2014) 237–251.
[57] F. Dakterzada, A.M. Mobarez, M.H. Roudkenar, A. Mohsenifar, Induction of humoral immune response against Pseudomonas aeruginosa flagellin (1-161) using gold nanoparticles as an adjuvant, Vaccine 34 (12) (2016) 1472–1479.
[58] Y. Wang, Y. Wang, N. Kang, Y. Liu, W. Shan, S. Bi, L. Ren, G. Zhuang, Construction and immunological evaluation of CpG-Au@ HBc virus-like nanoparticles as a potential vaccine, Nanoscale Res. Lett. 11 (1) (2016) 1–9.
[59] D. Rani, B. Nayak, S. Srivastava, Immunogenicity of gold nanoparticle-based truncated ORF2 vaccine in mice against Hepatitis E virus, 3 Biotech 11 (2) (2021) 1–11.
[60] S. Staroverov, N. Aksinenko, K. Gabalov, O. Vasilenko, I. Vidyasheva, S. Y. Shchyogolev, L. Dykman, Effect of gold nanoparticles on the respiratory activity of peritoneal macrophages, Gold Bull. 42 (2) (2009) 153–156.
[61] N.G. Bastús, E. Sánchez-Tilló, S. Pujals, C. Farrera, M.J. Kogan, E. Giralt, A. Celada, J. Lloberas, V. Puntes, Peptides conjugated to gold nanoparticles induce macrophage activation, Mol. Immunol. 46 (4) (2009) 743–748.
[62] H. Warren, F. Vogel, L. Chedid, Current status of immunological adjuvants, Annu. Rev. Immunol. 4 (1) (1986) 369–388.
[63] A. Shibaki, S. Katz, Induction of skewed Th1/Th2 T-cell differentiation via subcutaneous immunization with Freund's adjuvant, Exp. Dermatol. 11 (2) (2002) 126–134.
[64] L. Leroux, Z. Hatim, M. Freche, J. Lacout, Effects of various adjuvants (lactic acid, glycerol, and chitosan) on the injectability of a calcium phosphate cement, Bone 25 (2) (1999) 31S–34S.
[65] J.H. Eldridge, J.K. Staas, J.A. Meulbroek, T. Tice, R.M. Gilley, Biodegradable and biocompatible poly (DL-lactide-co-glycolide) microspheres as an adjuvant for staphylococcal enterotoxin B toxoid which enhances the level of toxin-neutralizing antibodies, Infect. Immun. 59 (9) (1991) 2978–2986.
[66] S. Marusic, S. Tonegawa, Tolerance induction and autoimmune encephalomyelitis amelioration after administration of myelin basic protein–derived peptide, J. Exp. Med. 186 (4) (1997) 507–515.
[67] V.L. Perez, L. Van Parijs, A. Biuckians, X.X. Zheng, T.B. Strom, A.K. Abbas, Induction of peripheral T cell tolerance in vivo requires CTLA-4 engagement, Immunity 6 (4) (1997) 411–417.
[68] M. Desmedt, P. Rottiers, H. Dooms, W. Fiers, J. Grooten, Macrophages induce cellular immunity by activating Th1 cell responses and suppressing Th2 cell responses, J. Immunol. 160 (11) (1998) 5300–5308.
[69] T. Kikuchi, R.G. Crystal, Antigen-pulsed dendritic cells expressing macrophage-derived chemokine elicit Th2 responses and promote specific humoral immunity, J. Clin. Investig. 108 (6) (2001) 917–927.
[70] A.K. Dey, A. Gonon, E.-I. Pécheur, M. Pezet, C. Villiers, P.N. Marche, Impact of gold nanoparticles on the functions of macrophages and dendritic cells, Cells 10 (1) (2021) 96.
[71] S. Ahmad, A.A. Zamry, H.-T.T. Tan, K.K. Wong, J. Lim, R. Mohamud, Targeting dendritic cells through gold nanoparticles: a review on the cellular uptake and subsequent immunological properties, Mol. Immunol. 91 (2017) 123–133.
[72] A. Sani, C. Cao, D. Cui, Toxicity of gold nanoparticles (AuNPs): a review, Biochem. Biophys. Rep. 26 (2021), 100991.
[73] A. Vartak, S.J. Sucheck, Recent advances in subunit vaccine carriers, Vaccines 4 (2) (2016) 12.
[74] L. Liu, Z. Liu, H. Chen, H. Liu, Q. Gao, F. Cong, G. Gao, Y. Chen, Subunit nanovaccine with potent cellular and mucosal immunity for COVID-19, ACS Appl. Bio Mater. 3 (9) (2020) 5633–5638.
[75] R. Itani, M. Tobaiqy, A. Al Faraj, Optimizing use of theranostic nanoparticles as a life-saving strategy for treating COVID-19 patients, Theranostics 10 (13) (2020) 5932.
[76] J. Machhi, F. Shahjin, S. Das, M. Patel, M.M. Abdelmoaty, J.D. Cohen, P.A. Singh, A. Baldi, N. Bajwa, R. Kumar, Nanocarrier vaccines for SARS-CoV-2, Adv. Drug Deliv. Rev. 171 (2021) 215–239.
[77] Y.H. Chung, V. Beiss, S.N. Fiering, N.F. Steinmetz, COVID-19 vaccine frontrunners and their nanotechnology design, ACS Nano 14 (10) (2020) 12522–12537.
[78] Y. Krishnamachari, S.M. Geary, C.D. Lemke, A.K. Salem, Nanoparticle delivery systems in cancer vaccines, Pharmaceut. Res. 28 (2) (2011) 215–236.